EXPERIMENTAL STUDY ON VARIABLE TEMPERATURE DRYING PROCESS OF PADDY BASED ON GLASS TRANSITION

/

基于玻璃化转变的稻谷变温干燥工艺及试验研究

Hongchao WANG [1]; Jing WANG [1]; Ziyu WANG *[2]; Lin WAN [1]; Gang CHE *[1]; Shuo WANG [1]; Zhengfa CHEN [1]

[1] College of Engineering, Heilongjiang Bayi Agricultural University, Daqing 163319, China

[2] College of Information and Electrical Engineering, Heilongjiang Bayi Agricultural University, Daqing 163319, China

Tel: 18645949778; E-mail: 295684617@qq.com

DOI: https://doi.org/10.35633/inmateh-76-88

Keywords: *paddy, variable-temperature drying, glass transition, experiment*

ABSTRACT

To improve the quality of paddy, reduce post-production losses, and ensure processing efficiency, this paper proposes a variable-temperature drying process based on the glass transition phenomenon, using the relationship between paddy moisture content and glass transition temperature. An optical three-dimensional scanning method was employed to obtain the paddy grain particle model. Subsequently, a heat and mass transfer model for paddy was constructed to analyze the temperature distribution and moisture migration behavior during drying. Experiments were conducted using a constant temperature of 40 ℃ and heating amplitudes of 5 ℃, 10 ℃, and 15 ℃ to investigate the drying characteristics and quality evolution of paddy. The simulation results showed that the average errors for moisture content and temperature were 1.58% and 2.66%, respectively. Compared with constant temperature drying at 40 ℃, the variable-temperature drying with heating amplitudes of 5 ℃, 10℃, and 15℃ reduced the drying time by 19, 58, and 63 minutes, respectively. Among the tested conditions, the 5 °C heating amplitude yielded the best results, with a crack increase rate of only 2.5% and a head rice yield of 68.3%. These findings offer valuable insights for understanding the mechanism of variable-temperature drying and for optimizing the drying process of paddy.

摘要

为提高稻谷品质、减少产后损失、保障加工质量等方面，本文通过稻谷含水率与玻璃化转变温度之间的关系，提出基于玻璃化转变的变温干燥工艺。采用光学三维扫描方法获取稻谷颗粒模型，再次基础上构建稻谷传热传质模型解析稻谷温度、水分的迁移规律。以 40℃恒温及 5℃、10℃、15℃的加热幅度为变量，开展试验探究稻谷干燥特性及其品质变化趋势。研究结果显示，模型模拟含水率的平均误差为 1.58%，温度的平均误差为 2.66%。与 40℃恒温干燥相比，5℃、10℃和 15℃升温幅度分别使干燥时间缩短了 19 分钟、58 分钟和 63 分钟。其中，5℃升温幅度的干燥工艺裂纹增率仅为 2.5%，整精米率达到 68.3%。研究结果为变温干燥机理及工艺优化提供参考。

INTRODUCTION

As one of the major staple foods in China, paddy production has remained above 200 million tons according to the 2024 national paddy production data released by the National Bureau of Statistics (*Islam et al., 2024*). However, annual post-harvest losses due to untimely or insufficient drying are estimated to be as high as 3–5% (*Tola et al., 2024*). Therefore, to prevent spoilage caused by mold, germination, and other deterioration processes, it is essential to dry and treat paddy promptly and adequately after harvest to ensure both yield and grain quality (*Zhang et al., 2024*).

Currently, hot-air drying is the most widely used method in commercial drying systems (*Okeyo et al., 2024*). It utilizes the temperature difference between hot air and the paddy to accelerate internal moisture evaporation. Using higher hot-air temperatures can effectively enhance drying efficiency (*Liu et al., 2024*).

However, if the temperature is not properly controlled, it may lead to a high incidence of grain cracking, which can severely impact the nutritional value and marketability of rice.

---

[1] *Hongchao Wang, Ph.D.*; *Jing Wang, master degree*; *Ziyu Wang, master degree*; *Lin Wan, Prof. Ph.D.*; *Gang Che, Prof. Ph.D.; Shuo Wang, Ph.D.*; *Zhengfa Chen, Ph.D.*

Paddy, as a polymeric material, undergoes a glass transition during the drying process due to temperature fluctuations (*Owusu et al., 2024*). When the temperature of the paddy is below its glass transition temperature, it enters a glassy state, characterized by low elasticity and high resistance to moisture diffusion. Conversely, at temperatures above the glass transition point, the grain enters a rubbery state, which exhibits higher elasticity and enhanced moisture diffusivity (*Wang et al., 2022*). Often, both glassy and rubbery states may coexist within the same grain, leading to internal structural changes and mechanical stress that may ultimately result in cracking. As temperature and moisture content vary throughout the drying process, the physical state of paddy dynamically shifts between the glassy and rubbery phases. According to the principles of glass transition, careful regulation of drying temperature to maintain a relatively stable physical state can significantly reduce the occurrence of cracking phenomena. While higher temperatures can maintain the rice in a rubbery state and promote rapid drying, they also increase the risk of cracking. In contrast, maintaining a glassy state through low-temperature drying helps minimize cracking but results in longer drying times and reduced efficiency (*Smith et al., 2024*). To balance drying efficiency and grain quality, variable-temperature hot-air drying has been widely adopted (*Rashid et al., 2023*). By adjusting the drying temperature over time, this approach helps minimize cracking while preserving post-drying grain quality (*Zhang et al., 2024*). However, the practical application of variable-temperature drying still faces several challenges, such as the accurate determination of temperature transition points and the prediction of quality changes during the process, which require further investigation and optimization.

Therefore, this study aims to establish a relationship between the glass transition temperature of paddy and moisture content and to analyze the coupled heat and mass transfer behavior during drying. By comparing constant-temperature drying with variable-temperature drying, the effects on drying characteristics, *head rice yield*, and crack increase rate are systematically explored.

MATERIALS AND METHODS

Experimental materials and equipment

In this experiment, paddy grains of the Suidao 3 variety from Heilongjiang Province were used. After harvesting in September 2024, the initial moisture content of the grains was approximately 22%. Following threshing, de-awning, and impurity removal, the paddy grains were sealed, packaged, and stored in a freezer at 2 ~ 4 °C for subsequent experiments. The hot-air drying experiment device was used in this study, as shown in Figure 1.

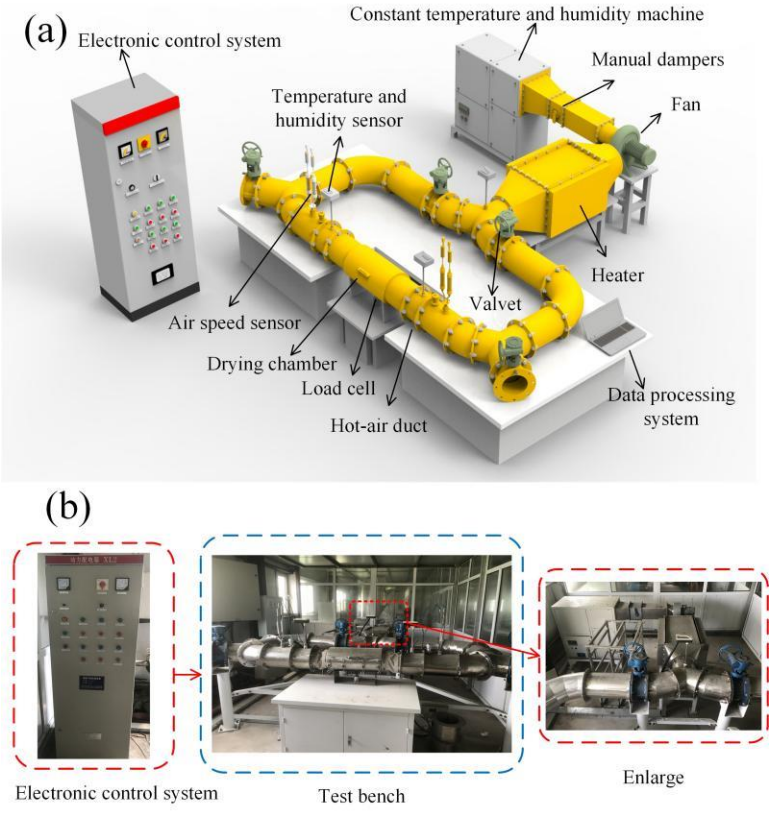

Fig. 1 - The hot-air drying experiment device

The device is capable of accurately controlling the temperature and air velocity, combined with a control system for recording and detecting data changes. The system is equipped with temperature and humidity sensors to dynamically detect the air temperature and humidity status at each pipe location, while the control unit makes rapid adjustments based on the set parameters. For each experiment, 200 grams of paddy were put into the drying area for processing. The hot air velocity was set at a constant 0.1 m/s, which remained constant throughout the drying process. A load cell was set at the bottom of the drying bin to continuously record the changes in sample mass.

Hot-air drying numerical simulation

Geometric modeling of paddy grain

In this study, the Suidao 3 variety was used as the test sample, and three-dimensional scanning technology was employed to obtain its geometric feature parameters. The test utilized an OKIO-5M 3D scanning device, which is based on the principle of structured light projection. The system captures the surface characteristics of the object using an image sensor and applies a phase resolution algorithm to accurately reconstruct the three-dimensional coordinate information of the sample surface. In the data processing stage, the raw point cloud data were processed with outlier removal and noise filtering, and then the morphological parameters of the sample were calculated, including the maximum projected area, equivalent volume and center of mass position. Subsequently, the final three-dimensional model is obtained for subsequent simulation operations by coloring, merging and correcting the model, as shown in Fig. 2.

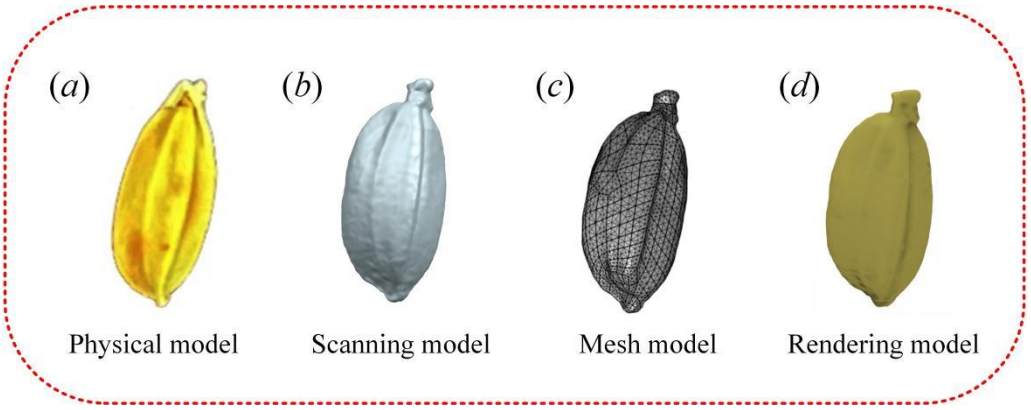

Fig. 2 - The three-dimensional geometric modeling of paddy grain

Model Assumptions

Modeling assumptions are required before numerical simulation modeling in this study (*Zhao et al., 2019*). (1) The paddy is regarded as an isotropic continuous medium material, and the initial state satisfies the conditions of uniform distribution of temperature and moisture in the paddy. (2) The drying process paddy diffuses in both liquid water and gaseous water. (3) Medium parameters in the drying process to maintain a steady state, ignoring the impact of fluctuations in environmental parameters (*Wang et al., 2024*).

Heat Transfer Equation

Based on the theory of energy conservation in a three-dimensional spatial coordinate system (x, y, z), the heat transfer phenomenon describing the hot-air drying process of paddy can be expressed by the following equations.

$$\rho C_p \frac{\partial T}{\partial t} = \lambda\left(\frac{\partial^2 T}{\partial x^2} + \frac{\partial^2 T}{\partial y^2} + \frac{\partial^2 T}{\partial z^2}\right) + h_g \rho \frac{\partial M}{\partial t} \quad (1)$$

The corresponding initial and boundary conditions are shown in equation (2).

$$\begin{cases} t = 0, \quad T = T_0 \\ -\lambda \dfrac{\partial T}{\partial t} = h_t\left(T - T_a\right) \end{cases} \quad (2)$$

where ρ is the density of paddy, (kg/m^3); C_p is the specific heat capacity of paddy, (J/kg·K); T is the temperature of paddy, ($^\circ$C); t is the time, (s); h_g is the latent heat of vaporization of paddy, (J/kg); M is the wet base moisture content of paddy, (kg/kg); T_0 is the initial temperature of paddy, (K); λ is the thermal conductivity of paddy, (W/m·K); T_a is the temperature of hot air, ($^\circ$C); h_t is the convective heat transfer coefficient, (W/m^2·K).

The h_t in the hot-air drying process can generally be calculated by the Nussel number (Nu), as shown in equation (3).

$$\begin{cases} Nu = \dfrac{h_t d}{\lambda_a} = 2 + 0.552\,\mathrm{Re}^{0.53}\,\mathrm{Pr}^{\left(\frac{1}{3}\right)} \\ \mathrm{Re} = \dfrac{v_a \rho_a d}{\mu_a} \\ Pr = \dfrac{\mu_a C_a}{\lambda_a} \end{cases} \quad (3)$$

where d is the equivalent diameter of paddy, (m); λ_a is the thermal conductivity of hot air, (W/m·K); Re is the Reynolds number; Pr is the Prandtl number; v_a is the velocity of hot air, (m/s); ρ_a is the density of hot air, (kg/m^3); μ_a is the dynamic viscosity of hot air, (Pa·s); C_a is the specific heat capacity of hot air, (J/kg·K).

Mass Transfer Equation

The heat transfer mechanism of hot-air drying of paddy covers convection and diffusion, and based on the mass conservation equation, the mathematical model of its internal moisture transport in a three-dimensional coordinate system can be described as follows:

$$\frac{\partial M}{\partial t} = D_{eff}\left(\frac{\partial^2 M}{\partial x^2} + \frac{\partial^2 M}{\partial y^2} + \frac{\partial^2 M}{\partial z^2}\right) \quad (4)$$

The initial and boundary conditions are set as follows:

$$\begin{cases} t = 0, \quad M = M_0 \\ -\lambda \dfrac{\partial M}{\partial t} = h_m\left(M - M_e\right) \end{cases} \quad (5)$$

where D_{eff} is the effective diffusion coefficient of moisture in paddy, (m^2/s); h_m is the convective mass transfer coefficient, (m/s); M_e is the equilibrium moisture content of paddy, (kg/kg); M_0 is the initial moisture content of paddy, (kg/kg).

The convective mass transfer coefficient (h_m) of paddy grain can generally be obtained by Sherwood number (Sh) calculation.

$$\begin{cases} Sh = \dfrac{h_m d}{D_a} = 2 + 0.552\,\mathrm{Re}^{0.53}\,Sc^{\left(\frac{1}{3}\right)} \\ Sc = \dfrac{\mu_a}{\rho_a D_a} \end{cases} \quad (6)$$

where D_a is the moisture diffusion coefficient in air, (m²/s); Sc is the Schmidt number.

Model solving

COMSOL Multiphysics software was used to select the fluid heat transfer and dilute matter transfer modules for the numerical simulation of the variable-temperature drying process of paddy. The grid independence was verified before solving, and the number and size of the grid were determined. The time step of the calculation was set to 10 seconds, and the simulation was done on a Dell 7810 workstation (Windows 10 system) equipped with 64 GB of RAM.

Experimental methods

Determination of glass transition temperature of paddy

Paddy samples weighing 500 g were randomly selected and dried under controlled conditions, with a constant temperature of 45 °C and a fixed air velocity of 0.5 m/s. The samples were taken at 10 min intervals and the moisture content was measured by a moisture meter, and then pulverized and placed in the refrigerator (2~4℃) for use. Paddy powders with different wet basis moisture content levels (10.1%, 12.5%, 14.3%, 16.2%, 18.3%, 20.4%, and 22.2%) were selected as test samples, and the glass transition temperature was determined by using a differential scanning calorimeter (*Chayjan et al., 2018*). Each sample with the same moisture content was tested three times, and the final glass transition temperature was obtained by averaging the results.

Variable-temperature hot-air drying experiment of Paddy

To investigate the influence of variable-temperature drying conditions on paddy drying quality, this study maintained a constant hot-air velocity and initial moisture content, while adjusting only the drying temperature during the variable-temperature experiments. The initial hot-air temperature was set at 40 °C, with temperature increments of 5 °C, 10 °C, and 15 °C applied in separate trials. Samples were taken at 10-minute intervals, and their moisture content was measured using a moisture meter until the safe storage standard of 14.0–14.5% was reached. When the moisture content of the paddy exceeded the value corresponding to the glass transition temperature by more than 4%, the drying temperature was increased to the next level according to the predefined increment. This protocol ensured that the paddy remained in the rubbery state throughout the entire drying process.

Indicator determination and calculation

Determination of initial moisture content of paddy refers to the use of grain, oilseed test Moisture Determination Method (GB/T 5497-1985), the paddy sample is placed in the drying box, and the weight of the paddy is measured several times at intervals of 1 h until the weight change is not more than 2 mg. The calculation of the wet-base moisture content of paddy at any moment of the drying process (M_t) is as shown in Equation (7) (*Nosrati et al., 2021*).

$$M_t = \frac{W_t - W_d}{W_t} \tag{7}$$

where W_t is the mass of the sample at time t, (g); t is the drying time, (s); W_d is the dry matter mass of the paddy sample, (g) (The paddy was dried at 105 °C until the change in weight was less than 0.02 g.).

The drying rate of paddy at different stages of the drying process was calculated by Equation (8).

$$DR = \frac{M_{t1} - M_{t2}}{t_2 - t_1} \tag{8}$$

where DR is the drying rate, (%/min); M_{t1} is the wet basis moisture content of paddy at time t_1, (%); M_{t2} is the wet basis moisture content of paddy at time t_2, (%).

After drying, the paddy was placed in a self-sealing bag and stored at room temperature for 48 h. It was then hulled, and the resulting brown rice was placed on a glass plate, where cracks were observed under a waist lamp. The cracking increase rate (F_{in}) was calculated according to equation (9).

$$F_{in} = \frac{n_f}{n} \tag{9}$$

where n is the number of paddy grains selected; n_f the number of paddy cracks.

The head rice yield was calculated according to equation (10).

$$HRY = \frac{m}{m_0} \times 100\% \tag{10}$$

where HRY is the head rice yield, (%); m_0 is the mass of paddy sample, (g); m is the mass of whole refined paddy, (g).

RESULTS AND DISCUSSIONS

Determination of the glass transition temperature of paddy

The glass transition curve of the Suidao 3 variety is shown in Fig. 3. This curve serves as a boundary that divides the paddy into two distinct physical states. In the region above the fitted curve, the paddy is in the rubbery state; conversely, in the region below the curve, the paddy is in the glassy state. By modeling this relationship, it becomes possible to predict and control the physical state of the paddy. Fluctuations in moisture content and temperature can cause transitions between these two states or maintain the current state, thereby influencing the physical and chemical properties of the paddy. This behavior aligns with the known plasticizing effect in polymeric materials, where a decrease in moisture content leads to an increase in the glass transition temperature. In this study, the variable-temperature drying process based on glass transition theory was defined to maintain the paddy in the rubbery state throughout the entire drying cycle (*Nasrnia et al., 2021*). As the moisture content of the paddy decreased from 22.2% to 10.1%, the glass transition temperature increased from 30.16 °C to 58.86 °C. A significant negative correlation was observed between the moisture content and the glass transition temperature.

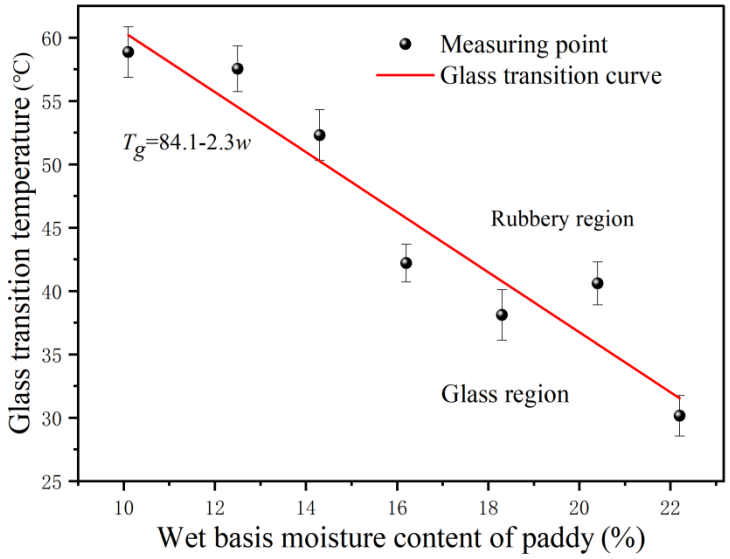

Fig. 3 - Fitted curve of moisture content and glass transition temperature for the Suidao 3 variety

Validation of the simulation model of paddy

Drying curves for the average moisture content and average temperature of paddy grains were obtained through numerical simulation. To ensure the accuracy of the comparison, the simulation and experimental drying conditions were kept consistent. The drying temperature was set to 45 °C, with an air velocity of 0.5 m/s. The comparison between the simulation and experimental results of the paddy drying process is shown in Fig. 4. As observed from the curves, paddy grains exhibited rapid moisture diffusion in the initial stage, followed by a slower diffusion rate as drying progressed. Meanwhile, the temperature of the paddy also rose rapidly, gradually reaching 45 °C. The simulated drying curves, derived from a three-dimensional scanning-based multi-physical field coupled model, showed a trend consistent with the experimental results. This indicates that the model effectively captures the changes in moisture and temperature during the drying process. The average error in simulated moisture content was 1.58%, with a mean square error of 0.11. For temperature, the average error was 2.66%, with an MSE of 1.35. According to previous studies, the acceptable error range for numerical simulations of paddy drying lies within 0–15% (*Zhao et al., 2019*). Therefore, the error range of the proposed model falls within acceptable limits, validating the accuracy and reliability of the established simulation model.

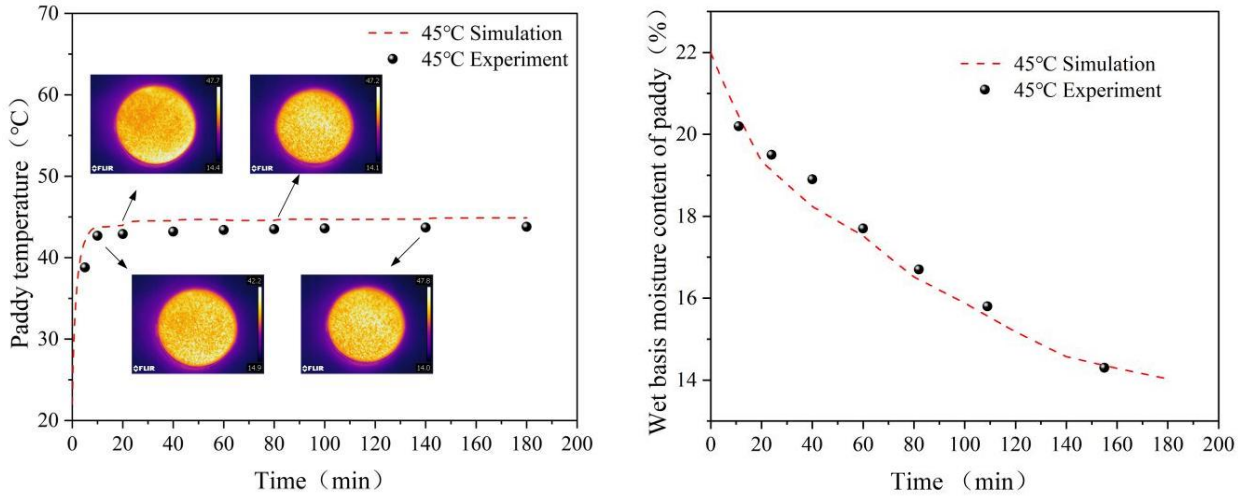

(a) Temperature variation of paddy (b) Moisture content variation of paddy

Fig. 4 - The comparison between the simulation and experimental results of the paddy drying process

Analysis of temperature and moisture changes in the paddy drying process

Under the initial conditions of an air velocity of 0.5 m/s and a moisture content of 22%, the drying process of paddy was simulated at a constant temperature of 40 °C, as well as with heating amplitude of 5 °C, 10 °C, and 15 °C. The internal temperature distributions of paddy grains under different drying conditions are shown in Fig. 5. At the initial stage of drying, the temperature of the paddy grains gradually increased upon exposure to hot air, eventually approaching the hot-air drying temperature asymptotically (*Li et al., 2024*). As shown in Fig. 5 (a)–(d), all four drying conditions maintained a grain surface temperature of approximately 40 °C at the 10-minute mark. The temperature of the outer layers increased more rapidly than that of the inner layers and progressively propagated inward. By the 30-minute mark, temperature differences among the four drying strategies began to emerge. In all cases, however, the outer layer temperature remained higher than that of the inner core. At 90 minutes, the internal temperature of the paddy grains approached the target drying temperature more closely across all test conditions. According to the law of conservation of energy, a portion of the input energy is consumed for moisture evaporation, resulting in the internal paddy temperature being slightly lower than the hot-air temperature throughout the process.

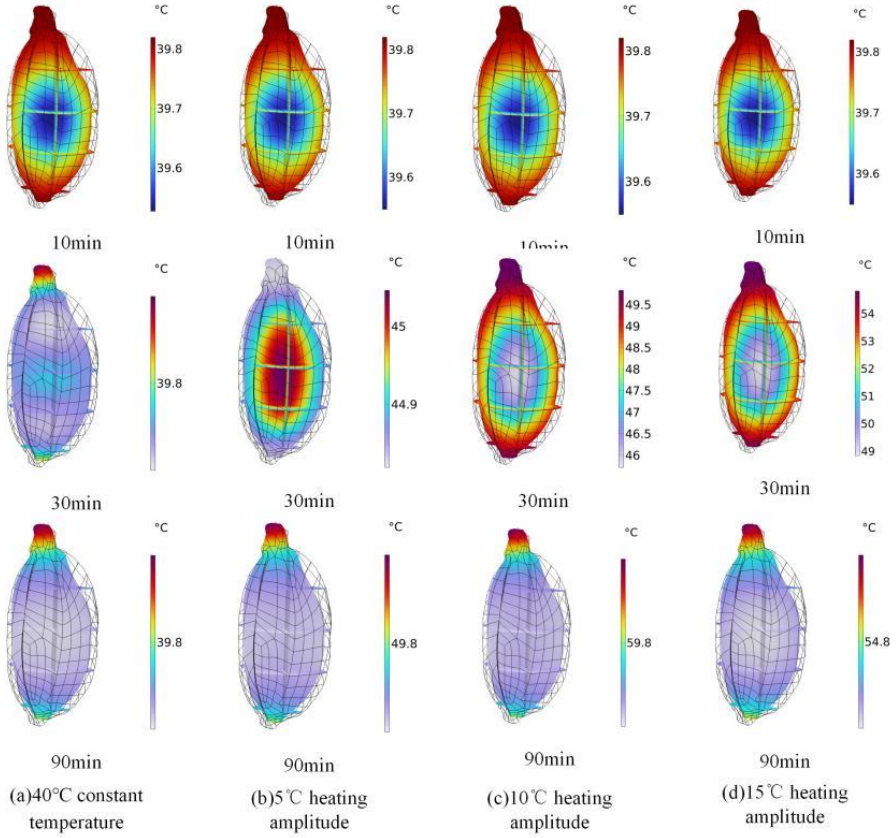

Fig. 5 - Internal temperature distribution of paddy under different hot-air drying conditions

Fig. 6 illustrates the internal moisture distribution of paddy under different hot-air drying conditions. Before the drying treatment, the internal temperature and moisture of the paddy grains were uniformly distributed. Moisture diffuses from the interior to the surface, which is the opposite direction of heat transfer (*Liu et al., 2022*). As shown in Figures 6(a)–(d), during the first 10 minutes of the drying process, the moisture distribution of all samples under the four drying conditions was generally consistent. During this initial stage, as the paddy grains came into contact with the hot air, internal moisture began to diffuse gradually toward the outer layers. By 30 minutes, the moisture distribution began to diverge across the different drying conditions. The rate and extent of internal moisture diffusion varied depending on the applied temperature gradient, resulting in noticeable differences in overall moisture content among the four treatments. At 90 minutes, during the later stage of drying, the internal moisture content of the grains decreased at a slower rate. The trends observed in the visualized moisture distribution were largely consistent with the experimental results, validating the accuracy of the simulation.

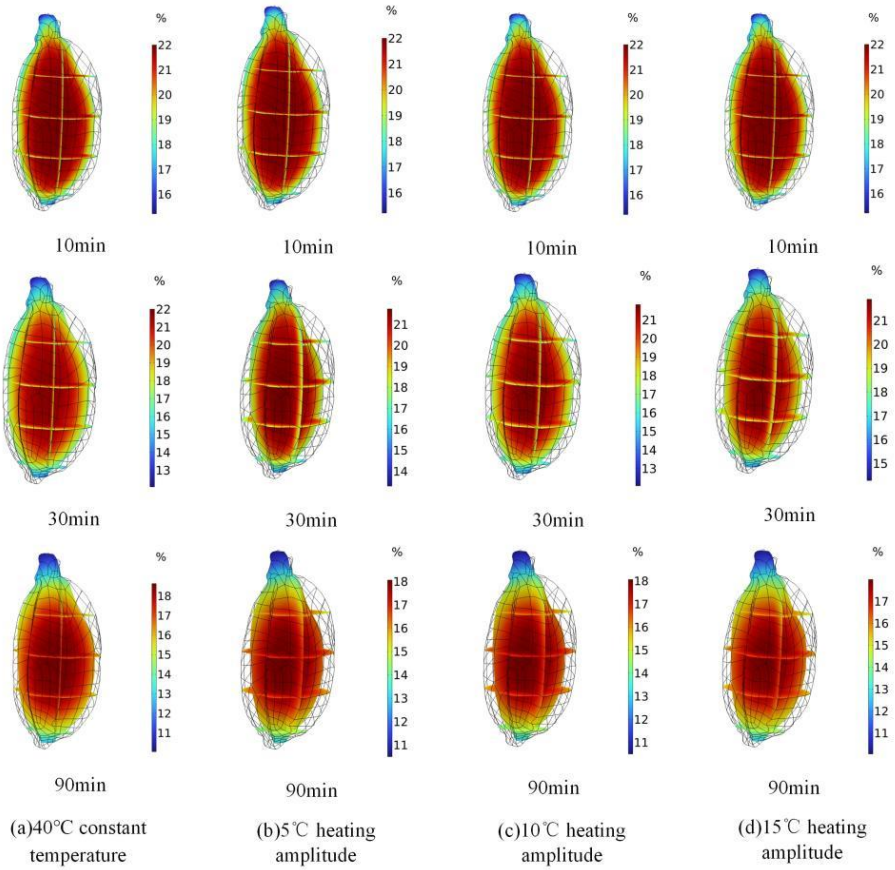

Fig. 6 - Internal moisture distribution of paddy grains under different hot-air drying conditions

Analysis of paddy drying characteristics

Fig. 7 illustrates the drying curves of paddy under different hot-air drying conditions.

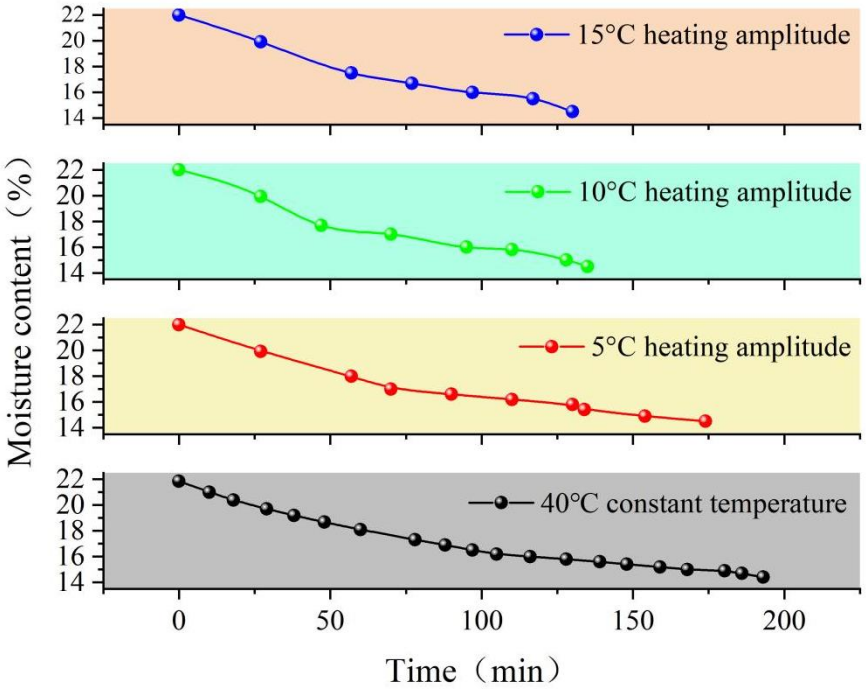

Fig. 7 - Drying curves of paddy under different hot-air drying conditions.

As shown in the figure, the moisture content exhibits a gradual decreasing trend. The turning point in the temperature change corresponds to the fitted curve of the glass transition temperature of the paddy. To ensure that the paddy remains in the rubbery state throughout the drying process, the initial drying temperature of 40 °C was followed by increases of 5 °C, 10 °C, and 15 °C in separate tests.

The longest drying time (174 min) was required when the air velocity was 0.5 m/s, the initial wet-base moisture content of paddy was 22%, and the heating amplitude was 5°C, while the shortest drying time (130 min) was required when the heating amplitude was 15°C. These results demonstrate that greater temperature increments lead to shorter drying durations. During the hot-air drying process, heat is transferred to the paddy primarily through convection and conduction. A temperature difference exists between the drying medium and the paddy, leading to heat absorption at the surface and its subsequent conduction into the interior. This promotes internal moisture evaporation. The larger the initial temperature increase, the greater the moisture gradient between the interior and exterior of the grain, resulting in a faster overall drying rate (*Guo et al., 2024*). This phenomenon can be attributed to the fact that, in the early stage of drying, the evaporation primarily involves non-bound water and moisture within the paddy husk. During this period, moisture diffusion and evaporation from the surface layer occur more rapidly, thereby accelerating the initial drying rate.

Fig.8 illustrates the drying rate curves of paddy under different hot-air drying conditions. As shown, the drying rate of paddy continuously changes throughout the drying process (*Sun et al., 2023*). In the initial stage, the drying rate increases rapidly due to the quick dissipation of surface moisture. In the middle and later stages, the drying rate exhibits minimal fluctuation. The fastest increase in drying rate was observed under the condition where the initial drying temperature was 40 °C with the heating amplitude of 15 °C. Conversely, when the heating amplitude was 5 °C, the drying rate increased at the slowest pace. During the constant-rate drying phase, differences in drying rate across conditions were relatively small. This is primarily due to the multi-layered structure of the paddy, which affects the evaporation and diffusion of moisture. At the beginning of the drying process, moisture in the paddy husk and non-bound water are removed first. Water diffuses from the interior of the grain to the surface and evaporates rapidly. As the moisture content decreases, internal water diffusion resistance increases, resulting in a decline in the drying rate during the later stages.

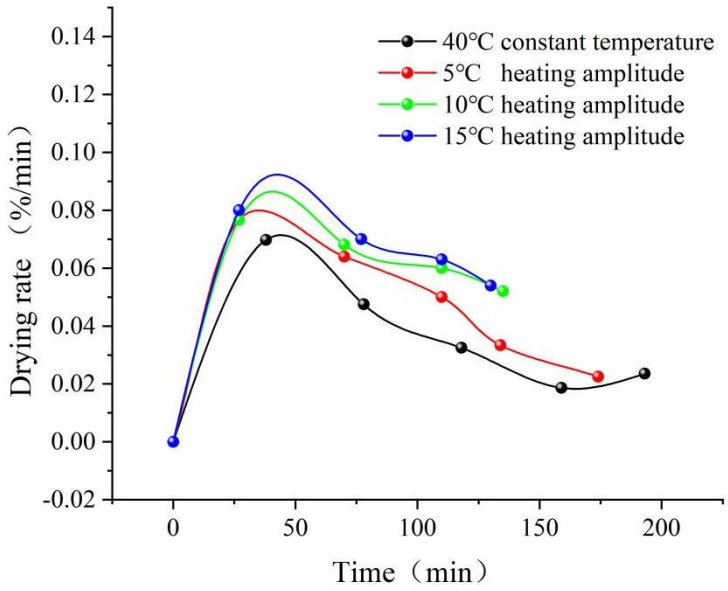

Fig. 8 - Drying rate curves of paddy under different hot-air drying conditions

Cracking increase rate

The effect of different hot-air drying conditions on the cracking increase rate of paddy is illustrated in Fig. 9. As shown in the figure, the cracking increase rate of paddy grain under varying drying conditions ranged from 2.5% to 6%. The cracking increase rate increased with the heating amplitude, reaching a maximum value of 6% under the drying condition with a 15 °C heating amplitude. It is noteworthy that when the cracking increase rate exceeds 3%, the paddy is more prone to breakage during the milling process, resulting in economic losses due to reduced yield of intact paddy. Compared to constant temperature drying at 40 °C, the drying condition with a 5 °C heating amplitude reduced the cracking increase rate by 0.3%. This indicates that variable temperature drying can effectively mitigate paddy cracking. The reduced cracking under the 5 °C heating amplitude is attributed to the absence of a glass transition in the paddy grain during drying, thereby minimizing internal stress and crack formation. However, when the heating amplitude increased to 10 °C and 15 °C, the cracking increase rate rose correspondingly. This trend is likely due to the development of more pronounced moisture gradients within the paddy grain at higher drying temperatures.

Even in the absence of a glass transition, these elevated gradients induce greater moisture stress, which in turn promotes cracking (*Mahmood et al., 2022*). Therefore, it can be concluded that excessive drying temperatures or large temperature increments are detrimental to paddy grain integrity. A carefully controlled heating range during hot air drying is crucial for minimizing grain cracking and ensuring post-processing quality.

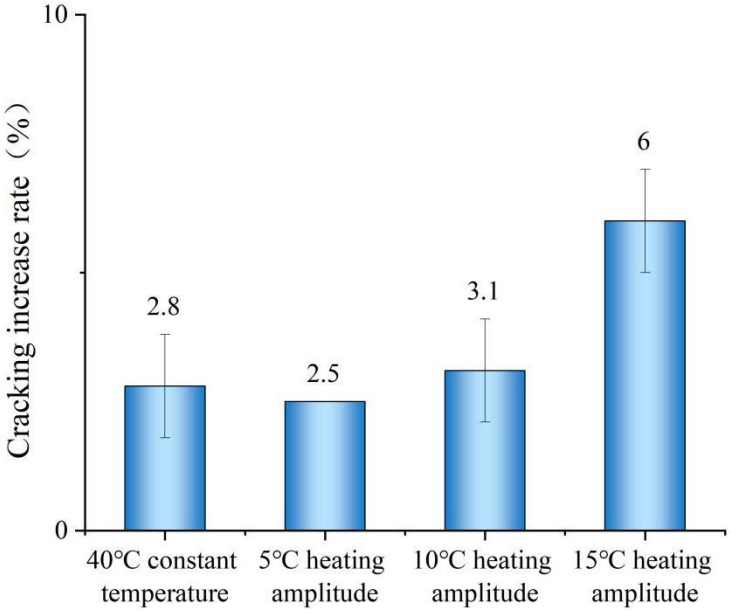

Fig. 9 - Effect of different hot-air drying conditions on the cracking increase rate of paddy

Head Rice Yield

Fig. 10 illustrates the effect of different hot-air drying conditions on the head rice yield of paddy. As shown in the figure, the HRY under various drying conditions ranged from 65.0% to 68.3%. Under the same initial drying temperature, a larger heating amplitude resulted in a lower HRY, with the maximum difference reaching 3.3%. This indicates a clear negative correlation between the temperature increase and head rice yield (*Mondal & Sarker, 2024*). The primary reason is that greater heating amplitudes lead to larger internal moisture gradients within the rice kernels, which promote grain fissuring during drying. These internal cracks increase the likelihood of grain breakage during milling, thereby reducing the final HRY. Compared to constant temperature drying at 40 °C, the HRY increased by 0.8% under a 5 °C heating amplitude. This result suggests that moderate variable-temperature drying can enhance the structural integrity of the grain and improve milling outcomes. HRY is not only a key indicator of the economic value of milled rice but also closely related to its sensory quality and nutritional attributes. Therefore, selecting optimal drying parameters, particularly in terms of heating amplitude, plays a vital role in maintaining and enhancing the processing quality of paddy.

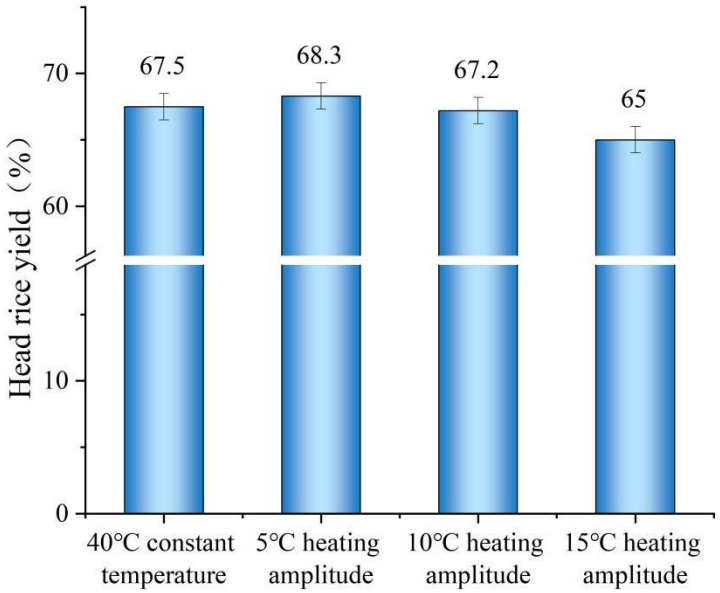

Fig. 10 - Effect of different hot-air drying conditions on the head rice yield of paddy

CONCLUSIONS

(1) Optical three-dimensional scanning was employed to obtain the three-dimensional geometric model of paddy. This method offers higher compatibility with the actual tri-axial dimensions of paddy and allows for a more realistic simulation of the drying process. By solving the heat and mass transfer models, the simulation of variable-temperature drying was successfully achieved. The simulation results showed high accuracy, with an average error of 1.58% and a mean square error of 0.11 for moisture content prediction, and an average error of 2.66% and MSE of 1.35 for temperature prediction.

(2) Glass transition curves were constructed based on the glass transition temperatures of paddy at different moisture contents. As the wet basis moisture content decreased from 22.0% to 10.1%, the glass transition temperature increased from 31.5 °C to 60.0 °C. Based on these curves, variable-temperature drying processes with heating amplitudes of 5 °C, 10 °C, and 15 °C were proposed. Compared with constant temperature drying, the variable-temperature drying processes reduced drying time by 19 min, 58 min, and 63 min, respectively. Among them, the process with a 5 °C heating amplitude showed the best performance, yielding a cracking increase rate of only 2.5% and a head paddy yield of 68.3%.

ACKNOWLEDGEMENT

This research was funded by the Daqing Municipal Directed Science and Technology Program, grant number zd-2025-032; the China Postdoctoral Science Foundation, grant number 2024MD763975; the School Orientation Training Research Initiation Fund Program, grant number XYB202307; the Heilongjiang Provincial Postdoctoral General Funding Project, grant number LBH-Z24250.

REFERENCES

[1] Chayjan R., Ghasemi A., & Sadeghi M. (2018). Stress fissuring and process duration during rough rice convective drying affected by continuous and stepwise changes in air temperature. *Drying Technology*, 37(2), 198-207. https://doi.org/10.1080/07373937.2018.1445637

[2] Guo, W., Cheng, S., Cui, Z., He, D., Zhang, X., Shi, T., & Du, J. (2024). Dynamic drying characteristics of alfalfa under solar energy-heat pump combined drying conditions. *INMATEH Agricultural Engineering*, 73(2), 569-580. https://doi.org/10.35633/inmateh-73-48

[3] Islam M. H., Momin A., Saha C. K., Alam M. M., & Islam S. (2024). Techno-economic analysis of BAU-STR dryer for rice drying: An approach to accelerate adoption. *Sustainability*, 16(22), 9846. https://doi.org/10.3390/su16229846

[4] Li X., Yang K., Wang Y., & Du X. (2024). Study on heat and moisture transfer of nonspherical rice during hot-air drying in thin-layer grain pile. *Journal of Food Process Engineering*, 47(4), e14597. https://doi.org/10.1111/jfpe.14597

[5] Liu H., He Y., Tang T., & Zhai M. (2022). Cracking prediction of germinated brown rice based on intragranular drying kinetics. *Powder Technology*, 406, 117587. https://doi.org/10.1016/j.powtec.2022.117587

[6] Liu Z., Che G., Wan L., Wang H., Chen Z., & Wang H. (2024). Design and experimental verification of self-priming hot air temperature changing device for grain dryer. *INMATEH Agricultural Engineering*, 73(2), 310-323. https://doi.org/10.35633/inmateh-73-26

[7] Mahmood N., Liu Y., Munir Z., Zhang Y., & Niazi B. (2022). Effects of hot air assisted radio frequency drying on heating uniformity, drying characteristics and quality of paddy. *Lwt-Food Science and Technology*, 158, 113131. https://doi.org/10.1016/j.lwt.2022.113131

[8] Mondal M., & Sarker M. (2024). Comprehensive energy analysis and environmental sustainability of industrial grain drying. Renewable and Sustainable *Energy Reviews*, 199, 114442. https://doi.org/10.1016/j.rser.2024.114442

[9] Nasrnia E., Sadeghi M., Raeisi Isa-Abadi A., & Mireei S. (2024). A novel simulation model to analyze rice intermittent drying considering glass transition concept. *Journal of Food Engineering*, 364, 111819. https://doi.org/10.1016/j.jfoodeng.2023.111819

[10] Nosrati M., Zare D., Nassiri S. M., Chen G., & Jafari A. (2021). Experimental and numerical study of intermittent drying of rough rice in a combined FIR-dryer. *Drying Technology*, 40(10), 1967-1979. https://doi.org/10.1080/07373937.2021.1898418

[11] Okeyo A. A., Luthra K., Vazquez A. R., & Atungulu G. G. (2024). Quality characteristic of instant rice produced using microwave-assisted hot air drying. *Cereal Chemistry*, 101(3), 641-653. https://doi.org/10.1002/cche.10770

[12] Owusu E. A., Luthra K., & Atungulu G. (2024). Material state diagrams for informed decision-making during drying of contemporary rice cultivars. *Drying Technology*, 42(5), 917-925. https://doi.org/10.1080/07373937.2024.2322110

[13] Smith D., Wason S., Atungulu G., & Bruce R. (2024). Radiofrequency (RF) drying of paddy rice and its effects on fissure formation and milling quality. *Applied Engineering in Agriculture*, 40(6), 697-714. https://doi.org/10.13031/aea.15966

[14] Rashid M. T., Liu K. L., Wei D. Z., Jatoi M. A., Li Q. Y., & Sarpong F. (2023). Drying kinetics and quality dynamics of ultrasound-assisted dried selenium-enriched germinated black rice. *Ultrasonics Sonochemistry*, 98, 106468. https://doi.org/10.1016/j.ultsonch.2023.106468

[15] Sun X., Guo Z., Wang G., Cai C., & Wang Z. (2023). Hot air drying, impact of infrared drying, and combined hot air-infrared drying on alfalfa drying quality and performance. *INMATEH Agricultural Engineering*, 71(3), 441-450. https://doi.org/10.35633/inmateh-71-38

[16] Wang C., Pei Y., Mu Z., Fan L., Kong J., Tian G., & Qiu H. (2024). Simulation analysis of 3-D airflow and temperature uniformity of paddy in a laboratory drying oven. *Foods*, 13(21), 3466. https://doi.org/10.3390/foods13213466

[17] Wang H., Che G., Wan L., & Tang H. (2022). Effects of drying approaches combined with variable temperature and tempering on the physicochemical quality of rice. *Drying Technology*, 41(7), 1199-1213. https://doi.org/10.1080/07373937.2022.2133140

[18] Zhang L., Jiang L., Adnouni M., Li S., & Zhang X. (2024). Numerical study on the variable-temperature drying and rehydration of shiitake. *Foods*, 13(21), 3356. https://doi.org/10.3390/foods13213356

[19] Zhang P., Li B., Hu Z., Zhang Q., Zhu Y., & Hao W. (2024). Effects of ultrasonic and microwave treatment on color, quality and drying characteristics of rice. *Journal of Cereal Science*, 116, 103856. https://doi.org/10.1016/j.jcs.2024.103856

[20] Zhao L., Yang J., Wang S., & Wu Z. (2019). Investigation of glass transition behavior in a rice kernel drying process by mathematical modeling. *Drying Technology*, 38(8), 1092-1105. https://doi.org/10.1080/07373937.2019.1612427